Quantitative Recognition of Granary Heat Source Using Quantum-Behaved Particle Swarm Optimization Method

Kun Wang,* Juan Liu,† Songtao Kong,‡ and Ping Cai§
Chongqing University of Science and Technology, 401331 Chongqing, People's Republic of China
Hongmei Xu¶
Chongqing Medical and Pharmaceutical College, 401331 Chongqing, People's Republic of China
and
Shibin Wan**
Chongqing University of Technology, 400054 Chongqing, People's Republic of China

https://doi.org/10.2514/1.T5885

On the basis of the inverse heat transfer methodology, the quantitative recognition of heat source parameters (location and intensity) in granary is studied using the finite element method and the quantum-behaved particle swarm optimization (QPSO) method. For the quantitative recognition problem of heat source parameters, a recognition system based on QPSO is established: the fitness function of QPSO is constructed according to the offsets between the measuring temperatures and calculating temperatures in granary, and the heat source parameters are obtained by optimizing the fitness function. The influence of heat source intensity, number of measuring points, measurement error, and initial guess value on the recognition results is studied through experiments, and compared with Levenberg–Marquardt method. The results show that the QPSO method in this paper can obviously weaken the influence of the number of measurement points and the initial guess on the recognition results and is able to ameliorate the anti-interference ability to the measurement errors.

Nomenclature

e	=	temperature deviation, °C
h	=	convective heat transfer coefficient, W/(m^2 · °C)
I	=	number of iteration
K	=	number of measurement points
k	=	index of the measurement point
$\boldsymbol{S}$	=	heat source parameter vector
r_d	=	heat source radius, mm
T, $\boldsymbol{T}$	=	temperature, temperature matrix, °C
$\boldsymbol{X}$	=	spatial position of the particles
$\boldsymbol{\Lambda}$	=	weighting matrix
λ	=	thermal conductivity, W/(m · °C)
σ	=	standard deviation of the measurement error, °C
ω	=	random number

Superscripts

cal	=	calculated
exa	=	exact

I. Introduction

BECAUSE of the damage of various types of grain storage facilities, the loss of grain production during storage remains a major problem worldwide [1]. Deficient rough rice storage management causes important grain damage every year [2]. Because of the high moisture content of the grain, insect pests, microbial reproduction, and seasonal atmospheric temperature, a heat source is formed in the granary, causing grain deterioration and even smoldering [3]. Maintaining a uniform temperature and moisture content during storage as well as early detection of heat sources so that appropriate action can be taken before major losses occur are important [4].

The heat source inside the object can be recognized by means of the inverse heat transfer problem (IHTP) method [5,6]. The information of the heat source (such as the location and intensity) inside the object is reflected in the distribution of the temperature field inside the object [7–9]. Furthermore, the quantitative recognition of heat sources in the granary can be achieved by the aid of temperature measurement information inside the granary during heat transfer process.

The IHTP is the estimation of some unknown characteristic parameters, such as boundary conditions, thermal physical parameters, geometry, internal defects, and source term, based on internal or surface temperature information of the heat transfer system [10–14]. The IHTP is widely used in scientific research and many technical fields, such as aerospace engineering [15,16], power engineering [17], materials processing [18], medical engineering [19], and nondestructive testing [20].

Many research results on the IHTP according to various optimization methods have been reported. Huang and Ozisik [21] used the conjugate gradient method (CGM) to identify the internal heat source intensity according to the plate wall temperature. Silva Neto and Özişik [22] simultaneously estimated the timewise-varying strengths of two plane heat sources using the conjugate gradient method. Le Niliot and Lefèvre [23] estimated the line heat sources by the parameter estimation approach. Mulcahy et al. [24] determined an unknown heat flux at an inner surface of the rocket when the outer surface temperature response was known from measurements using the steepest descent method (SDM). Miao and Liu [25] determined the source terms in the solid using SDM. Rouquette et al. [26] estimated the parameters of a Gaussian heat source with the Levenberg–Marquardt method (L-MM) during electron beam welding. CGM, SDM, and L-MM are gradient-based optimization algorithms, which belong to local optimization algorithm and are easy to fall into local

Received 18 August 2019; revision received 6 November 2019; accepted for publication 11 November 2019; published online 27 December 2019.

*Associate Professor, College of Mechanical and Power Engineering.
†Master, College of Mechanical and Power Engineering.
‡Professor, College of Mechanical and Power Engineering; stepsnow@126.com (Corresponding Author).
§Professor, College of Mechanical and Power Engineering.
¶Master, Higher Education Research Institute; xuhongmei01@foxmail.com.
**Master, School of Electrical and Electronic Engineering.

optimum, and their recognition results are easily influenced by the number of temperature points, the measurement errors, and the initial guesses.

The IHTP has an ill-posed characteristic [27]. The observation error of the temperature is likely to be magnified significantly in the inversion process, which leads to the instability of the inversion results. To solve the ill-posed problem of IHTP, several algorithms have been proposed. Ghosh et al. [28] estimated the location of internal heat source in conduction using an artificial neural network trained by a back-propagation (BP) algorithm and a genetic algorithm (GA) simultaneously. BP algorithm is not universal, and the recognition accuracy depends on the quantity of the sample data. Yang and Fu [29] identified the heat source as time-dependent using the Tikhonov regularization method. The inversion results of Tikhonov regularization method are decided by the precise choice of regularization parameters, but there is no universal method for precisely selecting regularization parameters in the absence of prior information on the inverse problem. Bhattacharya et al. [30] estimated the blast furnace reactor invisible interior surface using the differential evolution method, and the validity of the inversion method was proved by numerical experiments. However, in the traditional differential evolution method search process, it is difficult to determine the mutation operator accurately, which affects the accuracy and efficiency of inversion. Vakili and Gadala [31] solved the boundary inverse heat conduction problem in one, two, and three dimensions by particle swarm optimization (PSO), and the results showed that the PSO method can be applied to inverse heat conduction problem. But in the classical PSO algorithm, the convergence of particles is achieved by a certain trajectory and speed, and so the search space of each iteration step of particles is a limited area in the search process that cannot cover the whole feasible space, and thus the PSO algorithm may converge to the local optimal solution [32].

In quantum space, the aggregation of particles is accomplished by the bound states produced by some attractive potential in the center of particle motion. Particles in quantum bound states appear at any point in space with a certain probability density. Particles satisfying the aggregation properties can be searched in the entire feasible solution space, and so the quantum-behaved particle swarm optimization (QPSO) algorithm has a global convergence [33].

In this paper, the quantitative recognition system for heat source parameters of granary is established by employing finite element method (FEM) and QPSO method. The recognition system uses the temperature measurement information inside the granary, the fitness function of QPSO is constructed according to the offsets between the measuring temperatures and calculating temperatures in the granary, and the heat source parameters are obtained by optimizing the fitness function.

Here we discuss the influence of heat source intensity, number of measuring points, measurement error, and the initial guess value on the recognition results of heat source parameters, and compared with L-MM.

II. Heat Transfer Model with Internal Heat Source

The research object in the study is the cylindrical granary in Fig. 1. The granary is composed of grain and wall. There is convective heat transfer between the outer surface of the wall and the surrounding fluid. There is a heat source inside the granary.

For the convenience of discussion, it is assumed that the heat source is a sphere with radius r_d and the central coordinate of the heat source is (r_h, θ_h). The heat source intensity generated by the heat source per unit volume and time is represented by Φ_h.

The governing equations and solution conditions for heat transfer problems are, respectively, as follows:

$$\frac{1}{r}\frac{\partial}{\partial r}\left(\lambda r\frac{\partial T(r,\theta)}{\partial r}\right)+\frac{1}{r}\frac{\partial}{\partial \theta}\left(\lambda\frac{1}{r}\frac{\partial T(r,\theta)}{\partial \theta}\right)+\Phi_h=0$$
$$0\le r\le r_{\text{out}},\qquad 0\le\theta\le 2\pi \tag{1}$$

$$\lambda=\lambda_1\qquad 0\le r\le r_{\text{in}} \tag{2}$$

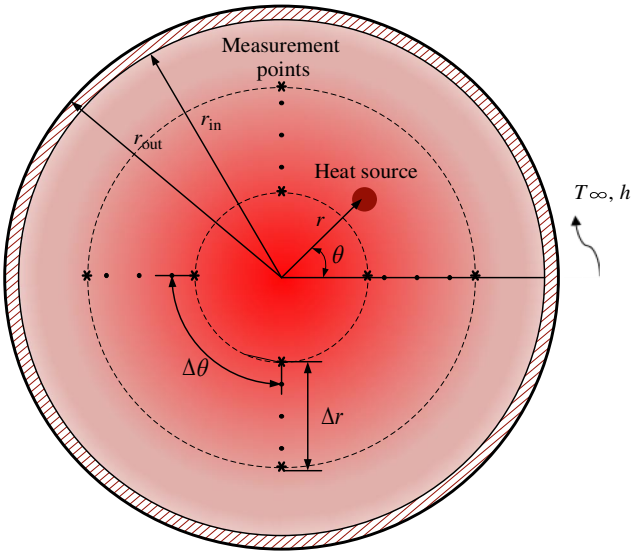

Fig. 1 Specimen with internal heat source.

$$\lambda=\lambda_2\qquad r_{\text{in}}\le r\le r_{\text{out}} \tag{3}$$

$$\lambda_1\left(\frac{\partial T(r,\theta)}{\partial r}\right)_{\text{inner}}=\lambda_2\left(\frac{\partial T(r,\theta)}{\partial r}\right)_{\text{outer}}\qquad r=r_{\text{in}} \tag{4}$$

$$-\lambda_2\frac{\partial T(r,\theta)}{\partial r}=h(T_{\text{out}}(\theta)-T_\infty)\qquad r=r_{\text{out}} \tag{5}$$

where λ_1 is the thermal conductivity of grain, λ_2 is the thermal conductivity of the granary wall, h is the convective heat transfer coefficient, and T_∞ is the ambient temperature.

If the parameter vectors of the internal heat source $\boldsymbol{S}=[r_h,\theta_h,\Phi_h]^T$ and the thermal boundary conditions of the granary are known, the temperature field $T(r,\theta)$ of the granary can be obtained according to the above heat transfer model. FEM is used to calculate $T(r,\theta)$ in this paper, and the heat conduction region is divided into $N_r\times N_\theta$ grids.

To verify the validity of the FEM model, the case of radial heat transfer with heat source problem is investigated in the present study. The heat transfer model, thermophysical parameter settings, and boundary conditions are the same as those in Ref. [34]. As shown in Fig. 2, it can be seen clearly that the results predicted by the FEM are in good agreement with the exact solution of Ref. [34], which indicates that the present FEM model could accurately predict the radial heat transfer problem.

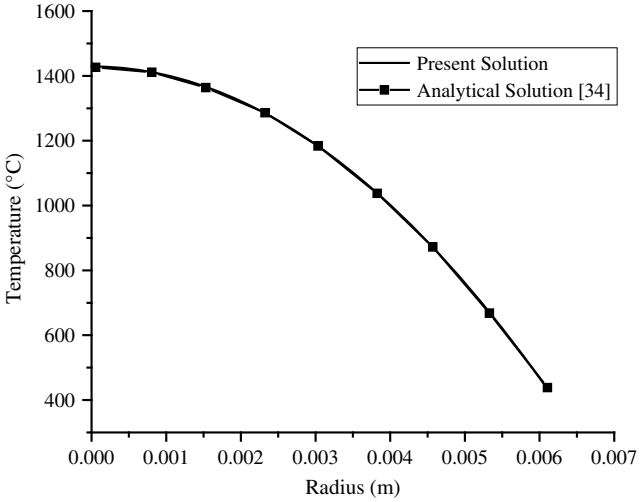

Fig. 2 Comparison between present computational solution and exact solution [34].

III. QPSO Scheme for Heat Source Parameters

A. Structure of the QPSO Recognition System

The QPSO recognition system shown in Fig. 3 is established to realize the recognition of the heat source parameters.

In Fig. 3, $T_k^{\text{mea}}(k = 1, 2, \ldots, K)$ represents the measuring temperature at the kth measuring point, and $T_k^{\text{cal}}(k = 1, 2, \ldots, K)$ represents the calculating temperature at the kth measuring point.

The objective function of the recognition system is constructed according to the residuals of the measuring and calculating temperatures inside the granary.

$$J(\boldsymbol{S}^i) = \sum_{k=1}^{K} [T_k^{\text{cal}}(\boldsymbol{S}^i) - T_k^{\text{mea}}]^2 \tag{6}$$

where $\boldsymbol{S}^i$ represents the ith estimation result of the heat source parameter vector $\boldsymbol{S} = [r_h, \theta_h, \Phi_h]^T$.

The recognition system takes the objective function as the fitness function of QPSO. By searching and optimizing the fitness function, the recognition result of the heat source parameter vector $\boldsymbol{S}$ can be obtained.

QPSO takes potential solutions of heat source parameters as particles in the search space. The spatial position of the particles can be expressed as follows:

$$\boldsymbol{X}_m^i = [x_{m,1}^i, x_{m,2}^i, \ldots, x_{m,N}^i] \qquad (m = 1, 2, \ldots, M) \tag{7}$$

where M is the number of particles; N is the dimension of solution space, that is, the dimension of the heat source parameters that needs to be estimated ($N = 3$); i is the number of iterations; and $x_{m,n}^i(n = 1, 2, \ldots, N)$ represent the nth-dimensional value of the mth particle.

Unlike standard PSO, particles in QPSO have no velocity vector, and the best position of an individual can be expressed as

$$\boldsymbol{P}_m^i = [p_{m,1}^i, p_{m,2}^i, \ldots, p_{m,N}^i] \tag{8}$$

where $p_{m,n}^i$ is the position of the mth particle corresponding to the n-dimensional solution space. $\boldsymbol{P}_m^i$ can be determined by Eq. (9):

$$\boldsymbol{P}_m^i = \begin{cases} \boldsymbol{X}_m^i & \text{if } J(\boldsymbol{X}_m^i) < J(\boldsymbol{P}_m^{i-1}) \\ \boldsymbol{P}_m^{i-1} & \text{if } J(\boldsymbol{X}_m^i) \geq J(\boldsymbol{P}_m^{i-1}) \end{cases} \tag{9}$$

Choose the best place of a group $\boldsymbol{P}_g^i = [p_{g,1}^i, p_{g,2}^i, \ldots, p_{g,N}^i]$, $[g \in (1, 2, \ldots, M)]$, and g can be determined by Eq. (10):

$$g = \arg \min_{1 \leq m \leq M} [J(\boldsymbol{P}_m^i)] \tag{10}$$

Take

$$q_{m,n}^i = \varphi_n^i \cdot p_{m,n}^i + (1 - \varphi_n^i) p_{g,n}^i \tag{11}$$

where φ_n^i is a uniformly distributed random number in interval [0, 1].

The evolution of particles can be expressed as

$$x_{m,n}^{i+1} = q_{m,n}^i \pm \alpha \cdot |C_n^i - x_{m,n}^i| \cdot \ell n(1/u_{m,n}^i) \tag{12}$$

where $u_{m,n}^i$ is the uniformly distributed random number in the interval [0, 1], α is the contraction-expansion (CE) coefficient, and C_n^i is the average of the best position of all the particles, which can be determined as follows:

$$C_n^i = \frac{1}{M} \sum_{m=1}^{M} p_{m,n}^i \tag{13}$$

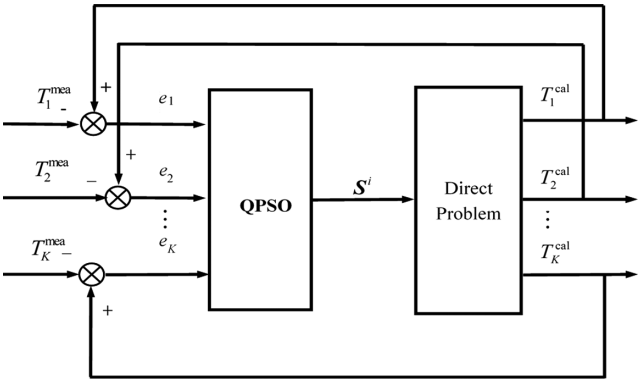

Fig. 3 Structure of QPSO recognition system.

B. Stopping Criterion of Iterations for Heat Source Parameters Recognition

The stopping criterion applied in the recognition process is shown as follows:

$$J(\boldsymbol{S}^i) = \sum_{k=1}^{K} [T_k^{\text{cal}}(\boldsymbol{S}^i) - T_k^{\text{mea}}]^2 \leq \varepsilon \tag{14}$$

where ε is a given decimal positive number.

C. Computational Process

The detailed process of estimating the heat source parameters is as follows:

1) Set $i = 1$, give the initial position $\boldsymbol{X}_m^1$ of the particle, and put the best position $\boldsymbol{P}_m^1 = \boldsymbol{X}_m^1$ of the individual.

2) Use formula (10) to determine the best location $\boldsymbol{P}_g^i$ of the group.

3) Take $\boldsymbol{S}^i = \boldsymbol{P}_g^i$, and solve the positive heat conduction problem to obtain the calculating temperature $T_k^{\text{cal}}(k = 1, 2, \ldots, K)$ at each measuring point.

4) If Eq. (14) is satisfied, the recognition process will end; otherwise the next step will be taken.

5) Calculate the position of the random point with formula (11).

6) Calculate the new position of the particles with formula (12).

7) Update the best position of individuals according to formula (9).

8) Set $i = i + 1$ and return to step 2.

IV. Numerical Experiments and Discussion

In the numerical experiment, the geometric parameters of the granary are $r_{\text{in}} = 12{,}200$ mm, $r_{\text{out}} = 12{,}500$ mm, and the radius of spherical heat source $r_d = 150$ mm (Fig. 1). The thermal conductivity of the grain is $\lambda_1 = 0.1052\,\text{W}/(\text{m} \cdot ^\circ\text{C})$ (moisture content was 10.8%) and that of the warehouse wall is $\lambda_2 = 1.74\,\text{W}/(\text{m} \cdot ^\circ\text{C})$. Convective heat transfer coefficient is $h = 8.0\ \text{W}/(\text{m}^2 \cdot ^\circ\text{C})$ and ambient fluid temperature is $T_\infty = 20^\circ\text{C}$.

Temperature measuring points are evenly arranged in the inner area of the granary along r and θ directions using formula (15) to generate simulation results of temperature measurements.

$$T_k^{\text{mea}} = T_k^{\text{exa}} + \omega\sigma \qquad (k = 1, 2, \ldots, K) \tag{15}$$

where T_k^{exa} is the "exact value" of the temperature at the measuring points by solving the positive problem based on the given heat source parameter vector $\boldsymbol{S}^{\text{exa}} = [r_h^{\text{exa}}, \theta_h^{\text{exa}}, \Phi_h^{\text{exa}}]^T$, ω is a set of random numbers within $[-2.576, 2.576]$ that obey the standard normal distribution, and σ is the standard deviation of the measurement error.

Table 1 Parameters of QPSO and FEM

Parameter	N_S	N_i	α	$N_r \times N_\theta$
Value	50	5000	[1, 0.4]	32×50

Without considering the measurement error (i.e., $\sigma = 0°C$), take $\varepsilon = 0.01$. When, take $\varepsilon = K\sigma^2$ according to the principle of deviation [35].

The QPSO method is used to realize quantitative recognition of the heat source parameters. The corresponding results are compared with those of L-MM [36]. To evaluate the availability of the above inverse methods, the relative errors of recognition results are defined.

$$\eta_r = |r_h^{\text{exa}} - r_h| / r_h^{\text{exa}} \times 100\% \tag{16a}$$

$$\eta_\theta = |\theta_h^{\text{exa}} - \theta_h| / \theta_h^{\text{exa}} \times 100\% \tag{16b}$$

$$\eta_\Phi = |\Phi_h^{\text{exa}} - \Phi_h| / \Phi_h^{\text{exa}} \times 100\% \tag{16c}$$

where r_h, θ_h, and Φ_h are the recognition results of the heat source parameters, and r_h^{exa}, θ_h^{exa}, and Φ_h^{exa} are the actual values of the corresponding parameters.

The number of QPSO particles N_s, the maximum number of iterations N_i, the contraction-expansion coefficient α, and the grid number $N_r \times N_\theta$ of FEM according to the validation results of grid independence are listed in Table 1.

A. Effect of Heat Source Intensity

Take the heat source parameters $\boldsymbol{S}_1^{\text{exa}} = [737, 312, 200]^T$, $\boldsymbol{S}_2^{\text{exa}} = [737, 312, 100]^T$, $\boldsymbol{S}_3^{\text{exa}} = [737, 312, 50]^T$. Choosing different heat source intensities, FEM is used to obtain the temperature distribution inside the granary, as shown in Fig. 4.

Take the range of heat source parameters $\Gamma = [-12, 500, 12, 500]$ for QPSO and the initial guesses of heat source parameters $\boldsymbol{S}^0 = [0, 0, 0]^T$ for L-MM in inversion process. The standard deviation of measurement error $\sigma = 0.1°C$. The number of measurement points $K = 64$. The simulation cases of QPSO are repeated for 50 trials to avoid the randomness of optimization results. When the actual heat source parameters were $\boldsymbol{S}_1^{\text{exa}}$, $\boldsymbol{S}_2^{\text{exa}}$, and $\boldsymbol{S}_3^{\text{exa}}$, the recognition results of QPSO and L-MM are shown in Figs. 5–7 and Table 2, respectively.

The diffusion characteristics of heat during heat transfer lead to the existence of high-temperature regions corresponding to heat sources in the granary. The greater the intensity of the heat source, the larger the high-temperature area is, and the greater the temperature difference between the high-temperature area and the surrounding area is. Figures 5–7 and Table 2 show that, when the intensity of heat source decreases, the temperature distribution difference of the measuring points inside the granary decreases and the recognition results of L-MM deteriorate obviously. QPSO is less sensitive to heat source intensity than L-MM and can improve the recognition accuracy of a low-intensity heat source.

B. Effect of the Number of Measurement Points

Take the heat source parameters $\boldsymbol{S}_1^{\text{exa}}$. The standard deviation of measurement error $\sigma = 0.1°C$. Take the range of heat source parameters $\Gamma = [-12, 500, 12, 500]$ for QPSO and the initial guesses of heat source parameters $\boldsymbol{S}^0 = [0, 0, 0]^T$ for L-MM in the inversion process. The number of measurement points is taken as $K = 64$, $K = 25$, and $K = 9$, respectively. The influence of the number of the temperature measurement points on the recognition results is

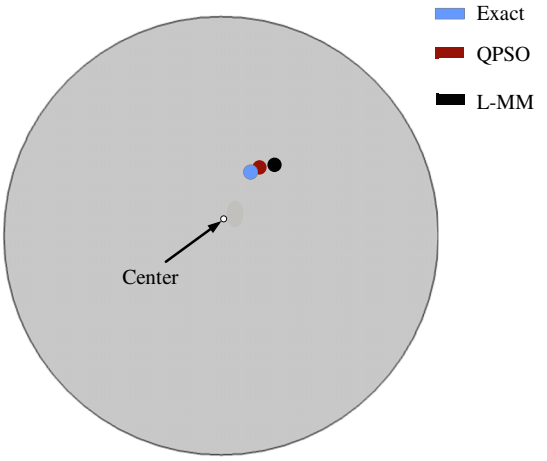

Fig. 5 Recognition results obtained by QPSO and L-MM using $\boldsymbol{S}_1^{\text{exa}}$.

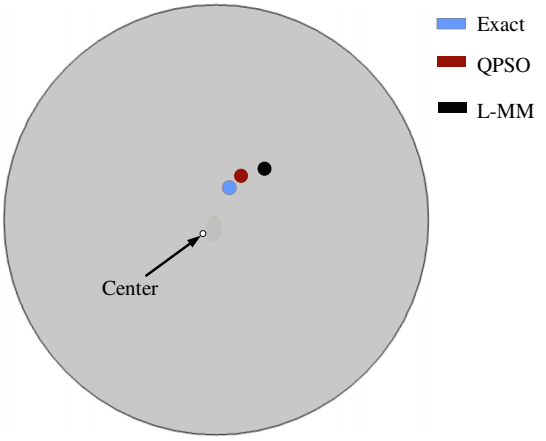

Fig. 6 Recognition results obtained by QPSO and L-MM using $\boldsymbol{S}_2^{\text{exa}}$.

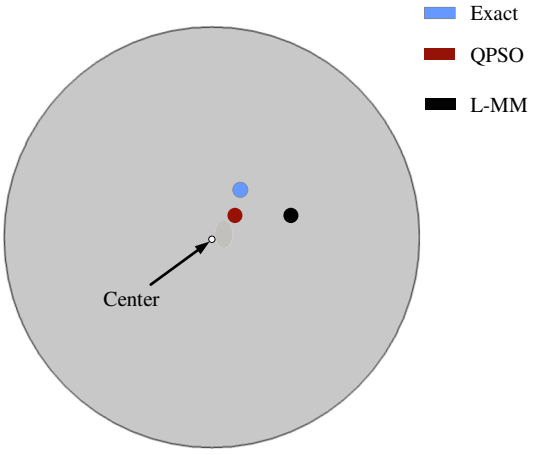

Fig. 7 Recognition results obtained by QPSO and L-MM using $\boldsymbol{S}_3^{\text{exa}}$.

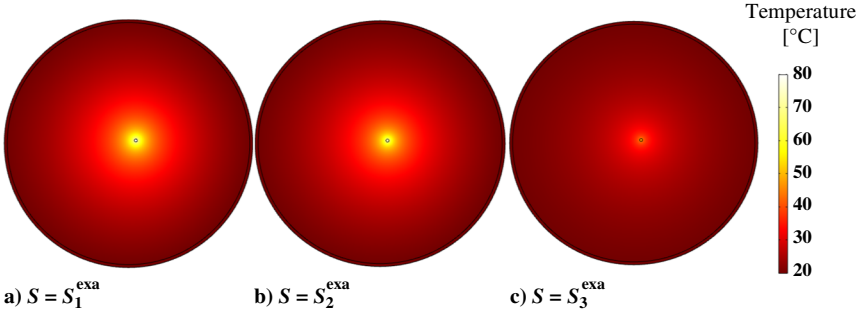

a) $S = S_1^{\text{exa}}$ **b) $S = S_2^{\text{exa}}$** **c) $S = S_3^{\text{exa}}$**

Fig. 4 Temperature distribution in the granary under different heat source intensities.

Table 2 Recognition results with different heat source intensity by QPSO and L-MM

Exact parameter	Method	Recognition result, mm			Relative error, %		
		r_h	θ_h	Φ_h	η_r	η_θ	η_Φ
$\boldsymbol{S}_1^{\text{exa}}$	QPSO	736.73	314.56	200.12	0.04	0.82	0.06
	L-MM	746.49	295.63	199.49	1.29	5.25	0.25
$\boldsymbol{S}_2^{\text{exa}}$	QPSO	730.59	323.11	99.82	0.86	3.56	0.18
	L-MM	773.01	275.84	100.58	4.89	11.59	0.58
$\boldsymbol{S}_3^{\text{exa}}$	QPSO	723.76	342.69	49.7	1.80	9.84	0.60
	L-MM	797.05	250.44	50.81	8.15	19.73	1.62

Table 3 Recognition results with different numbers of measurement points by QPSO and L-MM

K	Method	Recognition result, mm			Relative error, %		
		r_h	θ_h	Φ_h	η_r	η_θ	η_Φ
64	QPSO	739.67	301.62	200.42	0.36	3.33	0.21
	L-MM	746.49	295.63	199.49	1.29	5.25	0.25
25	QPSO	742.70	298.33	200.34	0.77	4.38	0.17
	L-MM	715.92	343.50	199.28	2.86	10.10	0.36
9	QPSO	725.97	330.88	199.46	1.50	6.05	0.27
	L-MM	794.28	241.52	202.51	7.77	22.59	1.25

investigated. The recognition results by QPSO and L-MM are shown in Table 3.

Table 3 shows that, when the number of measurement points decreases, the recognition result errors of L-MM increase obviously, but the QPSO recognition results are still satisfactory. The QPSO method depresses the influence of the number of measurement points on the recognition results in comparison with L-MM.

C. Effect of Measurement Errors

Take the heat source parameters $\boldsymbol{S}_1^{\text{exa}}$. The number of the measurement points is $K = 64$. Take the range of heat source parameters $\Gamma = [-12,500, 12,500]$ for QPSO and the initial guesses of heat source parameters $\boldsymbol{S}^0 = [0, 0, 0]^T$ for L-MM in the inversion process. To investigate the influence of the measurement error on the recognition results, the measurement error is increased. The recognition results by QPSO and L-MM are shown in Table 4.

Table 4 shows that the recognition results of QPSO are evidently better than those of L-MM when the temperature measurement errors are large. The QPSO method reduces the influence of the measurement errors on the recognition results and has strong anti-interference ability to the measurement errors. In addition, the maximum measurement error ($\sigma = 2$°C) has exceeded the error of common thermocouples in this temperature range [37], and the maximum relative error by QPSO method as high as 21.49% is barely satisfactory. As a result, the maximum tolerance measurement error $\sigma = 2$°C in this experiment.

D. Effect of Initial Guesses

Take the heat source parameters $\boldsymbol{S}_1^{\text{exa}}$. The number of measurement points is $K = 64$. The standard deviation of the measurement error is $\sigma = 0.1$°C. Take the range of heat source parameters $\Gamma = \beta[-12,500, 12,500]$ for QPSO and take the initial guesses of heat source parameters $\boldsymbol{S}^0 = \gamma \boldsymbol{S}_1^{\text{exa}}$ for L-MM in the inversion process. When different β and γ values are taken, the recognition results and relative errors of QPSO and L-MM methods are shown in Tables 5 and 6.

Table 4 Recognition results with different measurement errors by QPSO and L-MM

σ, °C	Method	Recognition result, mm			Relative error, %		
		r_h	θ_h	Φ_h	η_r	η_θ	η_Φ
0.5	QPSO	725.66	345.14	198.86	1.54	10.62	0.57
	L-MM	756.82	265.33	201.89	2.69	14.96	0.94
1.0	QPSO	705.29	355.96	201.21	4.30	14.09	0.61
	L-MM	804.13	252.83	204.35	9.11	18.96	2.17
2.0	QPSO	686.67	244.94	203.19	6.83	21.49	1.59
	L-MM	655.07	224.43	212.70	11.12	28.07	6.35

Table 5 Recognition results with different initial guesses by QPSO

β	Recognition result, mm			Relative error, %		
	r_h	θ_h	Φ_h	η_r	η_θ	η_Φ
0.06	728.49	319.77	199.61	1.15	2.49	0.19
0.6	726.95	322.05	200.84	1.36	3.22	0.42
1.0	739.67	301.62	200.42	0.36	3.33	0.21

Table 6 Recognition results with different initial guesses by L-MM

γ	Recognition result, mm			Relative error, %		
	r_h	θ_h	Φ_h	η_r	η_θ	η_Φ
0.0	746.49	295.63	199.49	1.29	5.25	0.25
0.25	739.82	301.28	199.91	0.39	3.44	0.05
0.75	735.71	313.01	200.19	0.18	0.32	0.10

Tables 5 and 6 show that when the initial guess value is close to the true value ($\beta = 0.06$, $\gamma = 0.75$), ideal recognition results can be obtained by L-MM and QPSO methods. Nevertheless, when the difference between the initial guess value and the real value is large ($\beta = 1.0$, $\gamma = 0.0$), the recognition results of L-MM deteriorate, whereas that of the QPSO method is still accurate, which means that QPSO is less affected by the initial guess.

V. Conclusions

In this paper, the QPSO recognition system is established for identifying the heat source parameters (position and intensity) in a granary. The effects of the heat source intensity, the number of temperature measurement points, the temperature measurement error, and the initial guess on the recognition results are discussed by numerical experiments.

The results show that QPSO can accurately recognize the heat source inside the granary. Compared with L-MM, QPSO weakens the influence of the initial guess and the number of measurement points on the recognition results, and enhances the anti-interference ability to the measurement errors.

Acknowledgments

This work was supported by the National Key R&D Program of China (2017YFC0805900); the Science and Technology Research Program of Chongqing Municipal Education Commission of China (KJQN201901526); and the Research Foundation of Chongqing University of Science & Technology of China (CK2016Z11).

References

[1] Huang, H., Danao, M. C., Rausch, K. D., and Singh, V., "Diffusion and Production of Carbon Dioxide in Bulk Corn at Various Temperatures and Moisture Contents," *Journal of Stored Products Research*, Vol. 55, Oct. 2013, pp. 21–26. https://doi.org/10.1016/j.jspr.2013.07.002

[2] Iguaz, A., Arroqui, C., Esnoz, A., and Vírseda, P., "Modelling and Validation of Heat Transfer in Stored Rough Rice Without Aeration," *Biosystems Engineering*, Vol. 88, No. 4, 2004, pp. 429–439. https://doi.org/10.1016/j.biosystemseng.2004.03.013

[3] Ogle, R. A., Dillon, S. E., and Fecke, M., "Explosion From a Smoldering Silo Fire," *Process Safety Progress*, Vol. 33, No. 1, 2014, pp. 94–103. https://doi.org/10.1002/prs.v33.1

[4] Asefi, M., Jeffrey, I., LoVetri, J., Gilmore, C., Card, P., and Paliwal, J., "Grain Bin Monitoring via Electromagnetic Imaging," *Computers and Electronics in Agriculture*, Vol. 119, Nov. 2015, pp. 133–141. https://doi.org/10.1016/j.compag.2015.10.016

[5] Chen, T., Cheng, C., Jang, H., and Tuan, P., "Using Input Estimation to Estimate Heat Source in Nonlinear Heat Conduction Problem," *Journal of Thermophysics and Heat Transfer*, Vol. 21, No. 1, 2007, pp. 166–172. https://doi.org/10.2514/1.22371

[6] Wu, N., Yang, R., Zhang, H., and Qiao, L., "Decentralized Inverse Model for Estimating Building Fire Source Location and Intensity," *Journal of Thermophysics and Heat Transfer*, Vol. 27, No. 3, 2013, pp. 563–575. https://doi.org/10.2514/1.T3976

[7] Lopes, D. D. C., Martins, J. H., Filho, A. F. L., Melo, E. D. C., Monteiro, P. M. D. B., and Queiroz, D. M. D., "Aeration Strategy for Controlling Grain Storage Based on Simulation and on Real Data Acquisition," *Computers and Electronics in Agriculture*, Vol. 63, No. 2, 2008, pp. 140–146. https://doi.org/10.1016/j.compag.2008.02.002

[8] Khatchatourian, O. A., Binelo, M. O., Neutzling, R., and , and Faoro, V., "Models to Predict the Thermal State of Rice Stored in Aerated Vertical Silos," *Biosystems Engineering*, Vol. 161, Sept. 2017, pp. 14–23. https://doi.org/10.1016/j.biosystemseng.2017.06.013

[9] Guo, S., Yang, R., Zhang, H., and Zhang, X., "New Inverse Model for Detecting Fire-Source Location and Intensity," *Journal of Thermophysics and Heat Transfer*, Vol. 24, No. 4, 2010, pp. 745–755. https://doi.org/10.2514/1.46513

[10] Wang, G., Zhu, L., and Chen, H., "A Decentralized Fuzzy Inference Method for Solving the Two-Dimensional Steady Inverse Heat Conduction Problem of Estimating Boundary Condition," *International Journal of Heat and Mass Transfer*, Vol. 54, Nos. 13–14, 2011, pp. 2782–2788. https://doi.org/10.1016/j.ijheatmasstransfer.2011.01.032

[11] Bozzoli, F., Mocerino, A., Rainieri, S., and Voscale, P., "Inverse Heat Transfer Modeling Applied to the Estimation of the Apparent Thermal Conductivity of an Intumescent Fire Retardant Paint," *Experimental Thermal and Fluid Science*, Vol. 90, Jan. 2018, pp. 143–152. https://doi.org/10.1016/j.expthermflusci.2017.09.006

[12] Huang, C. H., and Chao, B. H., "An Inverse Geometry Problem in Identifying Irregular Boundary Configurations," *International Journal of Heat and Mass Transfer*, Vol. 40, No. 9, 1997, pp. 2045–2053. https://doi.org/10.1016/S0017-9310(96)00280-3

[13] Wang, K., Wang, G., Chen, H., Wan, S., and Lv, C., "Quantitative Identification of Three-Dimensional Subsurface Defect Based on the Fuzzy Inference of Thermal Process," *International Journal of Heat and Mass Transfer*, Vol. 133, April 2019, pp. 903–911. https://doi.org/10.1016/j.ijheatmasstransfer.2018.12.149

[14] Sun, S., Qi, H., Zhao, F., Ruan, L., and Li, B., "Inverse Geometry Design of Two-Dimensional Complex Radiative Enclosures Using Krill Herd Optimization Algorithm," *Applied Thermal Engineering*, Vol. 98, April 2016, pp. 1104–1115. https://doi.org/10.1016/j.applthermaleng.2016.01.017

[15] Walker, D. G., and Scott, E. P., "Evaluation of Estimation Methods for High Unsteady Heat Fluxes from Surface Measurements," *Journal of Thermophysics and Heat Transfer*, Vol. 12, No. 4, 1998, pp. 543–551. https://doi.org/10.2514/2.6374

[16] Chanda, S., Balaji, C., Venkateshan, S. P., Yenni, G. R., and Ambirajan, A., "Joint Conductance Effects on Estimation of Effective Thermal Conductivities of Anisotropic Composites," *Journal of Thermophysics and Heat Transfer*, Vol. 28, No. 3, 2014, pp. 553–560. https://doi.org/10.2514/1.T4276

[17] Wang, K., Wang, G., Chen, H., and Zhu, L., "Estimating Thermal Boundary Conditions of Boiler Membrane Water-Wall Using Decentralized Fuzzy Inference with Sensitivity Weighting," *Applied Thermal Engineering*, Vol. 66, Nos. 1–2, 2014, pp. 309–317. https://doi.org/10.1016/j.applthermaleng.2014.02.020

[18] Ning, J., Sievers, D. E., Garmestani, H., and Liang, S. Y., "Analytical Modeling of Transient Temperature in Powder Feed Metal Additive Manufacturing During Heating and Cooling Stages," *Applied Physics A*, Vol. 125, No. 8, 2019. https://doi.org/10.1007/s00339-019-2782-7

[19] Bezerra, L. A., Oliveira, M. M., Rolim, T. L., Conci, A., Santos, F. G. S., Lyra, P. R. M., and Lima, R. C. F., "Estimation of Breast Tumor Thermal Properties Using Infrared Images," *Signal Processing*, Vol. 93, No. 10, 2013, pp. 2851–2863. https://doi.org/10.1016/j.sigpro.2012.06.002

[20] Huang, C., and Chaing, M., "A Thermal Tomography Problem in Estimating the Unknown Interfacial Enclosure in a Multiple Region Domain with an Internal Cavity," *Computer Modeling in Engineering & Sciences*, Vol. 53, No. 2, 2009, pp. 153–179. https://doi.org/10.3970/cmes.2009.053.153

[21] Huang, C. H., and Ozisik, M. N., "Inverse Problem of Determining the Unknown Strength of an Internal Plane Heat Source," *Journal of the Franklin Institute*, Vol. 329, No. 4, 1992, pp. 751–764. https://doi.org/10.1016/0016-0032(92)90086-V

[22] Silva Neto, A. J., and Özişik, M. N., "Inverse Problem of Simultaneously Estimating the Timewise-Varying Strengths of Two Plane Heat Sources," *Journal of Applied Physics*, Vol. 73, No. 5, 1993, pp. 2132–2137. https://doi.org/10.1063/1.353160

[23] Le Niliot, C., and Lefèvre, F., "A Parameter Estimation Approach to Solve the Inverse Problem of Point Heat Sources Identification," *International Journal of Heat and Mass Transfer*, Vol. 47, No. 4, 2004, pp. 827–841. https://doi.org/10.1016/j.ijheatmasstransfer.2003.08.011

[24] Mulcahy, J. M., Browne, D. J., Stanton, K. T., Chang Diaz, F. R., Cassady, L. D., Berisford, D. F., and Bengtson, R. D., "Heat Flux Estimation of a Plasma Rocket Helicon Source by Solution of the Inverse Heat Conduction Problem," *International Journal of Heat and Mass Transfer*, Vol. 52, Nos. 9–10, 2009, pp. 2343–2357. https://doi.org/10.1016/j.ijheatmasstransfer.2008.10.031

[25] Miao, X., and Liu, Z., "Two Dimensional Determination of Source Terms in Linear Parabolic Equation from the Final Overdetermination," *Advances in Difference Equations*, Vol. 2015, No. 1, 2015, p. 98. https://doi.org/10.1186/s13662-015-0401-2

[26] Rouquette, S., Guo, J., and Le Masson, P., "Estimation of the Parameters of a Gaussian Heat Source by the Levenberg–Marquardt Method: Application to the Electron Beam Welding," *International Journal of Thermal Sciences*, Vol. 46, No. 2, 2007, pp. 128–138. https://doi.org/10.1016/j.ijthermalsci.2006.04.015

[27] Beck, J. V., Blackwell, B., and St. Clair, C. R., Jr., *Inverse Heat Conduction Ill-Posed Problems*, Wiley, New York, 1985, pp. 108–112.

[28] Ghosh, S., Pratihar, D. K., Maiti, B., and Das, P. K., "Inverse Estimation of Location of Internal Heat Source in Conduction," *Inverse Problems in Science and Engineering*, Vol. 19, No. 3, 2011, pp. 337–361. https://doi.org/10.1080/17415977.2011.551876

[29] Yang, F., and Fu, C., "The Method of Simplified Tikhonov Regularization for Dealing with the Inverse Time-Dependent Heat Source Problem," *Computers & Mathematics with Applications*, Vol. 60, No. 5, 2010, pp. 1228–1236. https://doi.org/10.1016/j.camwa.2010.06.004

[30] Bhattacharya, A. K., Aditya, D., and Sambasivam, D., "Estimation of Operating Blast Furnace Reactor Invisible Interior Surface Using Differential Evolution," *Applied Soft Computing*, Vol. 13, No. 5, 2013, pp. 2767–2789. https://doi.org/10.1016/j.asoc.2012.10.010

[31] Vakili, S., and Gadala, M. S., "Effectiveness and Efficiency of Particle Swarm Optimization Technique in Inverse Heat Conduction Analysis," *Numerical Heat Transfer, Part B: Fundamentals*, Vol. 56, No. 2, 2009, pp. 119–141. https://doi.org/10.1080/10407790903116469

[32] Van den Bergh, F., *An Analysis of Particle Swarm Optimizers*, Univ. of Pretoria, Pretoria,, South Africa, 2011, pp. 107–113.

[33] Sun, J., Wu, X., Palade, V., Fang, W., Lai, C., and Xu, W., "Convergence Analysis and Improvements of Quantum-Behaved Particle Swarm Optimization," *Information Sciences*, Vol. 193, June 2012, pp. 81–103. https://doi.org/10.1016/j.ins.2012.01.005

[34] Kim, H. T., Rhee, B. W., and Park, J. H., "Application of the Finite Volume Method to the Radial Conduction Model of the CATHENA Code," *Annals of Nuclear Energy*, Vol. 33, No. 10, 2006, pp. 924–931. https://doi.org/10.1016/j.anucene.2006.04.011

[35] Alifanov, O. M., "Solution of an Inverse Problem of Heat Conduction by Iteration Methods," *Journal of Engineering Physics*, Vol. 26, No. 4, 1974, pp. 471–476. https://doi.org/10.1007/BF00827525

[36] Fan, C., Sun, F., and Yang, L., "A General Quantitative Identification Algorithm of Subsurface Defect for Infrared Thermography," *2005 Joint 30th International Conference on Infrared and Millimeter Waves and 13th International Conference on Terahertz Electronics*, IEEE, New York, Sept. 2005. https://doi.org/10.1109/ICIMW.2005.1572552

[37] "Thermocouple Types," Omega Engineering, Inc., https://www.omega.com/en-us/resources/thermocouple-types [retrieved 7 Nov. 2019].